

UDK 57.012.3

## Mechanical Properties and Microstructure of Al<sub>2</sub>O<sub>3</sub>/TiAl in Situ Composites Doped with Cr and V<sub>2</sub>O<sub>5</sub>

**Kun Zhang\*, Wang Fen, Jianfeng Zhu, Huae Wu**

Key Laboratory of Auxiliary Chemistry & Technology for Chemical Industry,  
Ministry of Education, Shaanxi University of Science & Technology,  
Xi'an, 710021, China

---

### **Abstract:**

*Al<sub>2</sub>O<sub>3</sub>/TiAl in situ composites doped with Cr and V<sub>2</sub>O<sub>5</sub> were successfully prepared from Ti, Al, TiO<sub>2</sub>, Cr and V<sub>2</sub>O<sub>5</sub> by hot pressing. The effect of in situ formed Al<sub>2</sub>O<sub>3</sub> content on the phase composition, microstructure and mechanical properties of Al<sub>2</sub>O<sub>3</sub>/TiAl composites were investigated. The results show that the as-synthesized composites mainly consisted of  $\gamma$ -TiAl/ $\alpha_2$ -Ti<sub>3</sub>Al matrix and dispersive Al<sub>2</sub>O<sub>3</sub> reinforcing phases. The in situ formed fine Al<sub>2</sub>O<sub>3</sub> ceramic particles mainly disperse on the grain boundaries of TiAl, resulting in refinement of TiAl matrix, which improves the mechanical properties of the Al<sub>2</sub>O<sub>3</sub>/TiAl in situ composite. The composite with 7.54 at.% Al<sub>2</sub>O<sub>3</sub> possesses the maximum flexural strength and fracture toughness of 335.38 MPa and 5.39 MPa m<sup>1/2</sup>, respectively. The strengthening mechanism was also discussed in detail.*

**Keywords:** TiAl composites, Al<sub>2</sub>O<sub>3</sub>, Microstructure, Mechanical properties

---

### **1. Introduction**

The TiAl-based alloy ( $\gamma$ -TiAl+ $\alpha_2$ -Ti<sub>3</sub>Al) is particularly attractive for their high melting point, low density, high specific strength, high elastic ratio, good oxidation resistance, relatively good properties at elevated temperatures and high creep resistance at temperatures up to 1000°C, and have received considerable interest to various applications in the aerospace, automotive, and energy production industries [1-5]. The factors that limit the alloys from widespread use include low room temperature ductility and elevated temperature formability. Nowadays researches have focused on the production of ultrafine grained TiAl and second-phase particles reinforcement in attempt to improve the ductility [6-10]. Recently, several methods have been applied to fabricate the TiAl matrix composites, such as hot isostatic pressing, spark plasma sintering, reactive sintering, mechanical alloying, vacuum arc remelting and powder metallurgy [11-16].

The combination of in situ synthesis with vacuum hot press sintering is a very viable approach to prepare Al<sub>2</sub>O<sub>3</sub>/TiAl composites. It could not only maintain the super inherent properties of the TiAl matrix, but also improve other properties by the formation of the reinforcements (such as TiB<sub>2</sub>, SiC, TiC, Ti<sub>2</sub>AlC and Al<sub>2</sub>O<sub>3</sub>). It represents an in situ processing technique for the fabrication of composites, which takes the advantage of low energy requirement, cleaner particle-matrix interface, and one step forming process, dense and high purity of the products [17, 18]. Owing to its excellent thermo-mechanical behavior (including

---

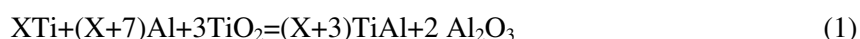
\*) Corresponding author: sifan279318474@163.com

wear resistance, environmental stability, and high temperature strength) and close match of the thermal expansion coefficient with that of  $\gamma$ -TiAl,  $\text{Al}_2\text{O}_3$  ceramic particle is selected as reinforcement compared with other ceramic phases. Additionally, micro-alloying can be used to improve fracture resistance and ductility.

Former studies have demonstrated that V and Cr could effectively improve the properties of TiAl materials but optimization of alloying elements content was not mentioned specifically. Therefore, in situ synthesis was planned to adopt in order to further develop properties of the alloying materials [19].

## 2. Experimental procedure

For fabrication of the in situ  $\text{Al}_2\text{O}_3/\text{TiAl}$  composites, commercially available powders of Ti (280 mesh, 99.3% purity), Al (200 mesh, 99.5% purity),  $\text{TiO}_2$  (0.5  $\mu\text{m}$ , 99% purity), Cr (320 mesh, 99% purity) and  $\text{V}_2\text{O}_5$  (400 mesh, 99.0% purity) were utilized as starting materials. The powders were mixed with the expected compositions according to the stoichiometry of the following reaction formula 1, in addition, 1.25 at.%  $\text{V}_2\text{O}_5$  and 1.0 at.% Cr were added, respectively. The specific constituent of the samples was listed in Tab. I.



The elemental powder blends were ball milled in alcohol in alumina jars for 1.5 h, and the mass ratio of powder, alcohol and alumina ball is 1:1:3. The powders were sifted with a 200 mesh, dried at 35 °C for several hours, compacted under 10 MPa in a graphite mold, and then sintered in a hot-press furnace in vacuum of  $1 \times 10^{-2}$  Pa. The compacted samples were first heated from room temperature to 500 °C for 1h from 500 °C to 900 °C for 1h from 900 °C to 1250 °C for 1.5 h, and then held at 1250 °C for 2 h under a uniaxial pressure of 20 MPa. Finally, the products were cooled down to room temperature in the furnace.

**Tab. I.** The component of the  $\text{Al}_2\text{O}_3/\text{TiAl}$  composites (at.%)

Samples No.	Ti	Al	$\text{TiO}_2$	$\text{V}_2\text{O}_5$	Cr	Target $\text{Al}_2\text{O}_3$
a	44.33	50.69	2.73	1.25	1.0	3.86
b	39.66	52.56	5.52	1.25	1.0	7.54
c	34.88	54.47	8.40	1.25	1.0	11.45

The as-fabricated specimens were polished by automatic pre-milling machine to take off contaminants. The hardness of  $\text{Al}_2\text{O}_3/\text{TiAl}$  composites with different contents of  $\text{Al}_2\text{O}_3$  was measured in an HXD-1000 tester (at a 10 N load for 15 s) and density was tested by the Archimedes method.

Three point bending tests were performed to measure flexural strength and fracture toughness ( $K_{IC}$ ) at room temperature on a universal testing machine (PT-1036PC, Perfect Instrument Co. Ltd, Taiwan China). Specimens with dimensions of  $30 \times 4 \times 4 \text{ mm}^3$  polished accurately to 1  $\mu\text{m}$  were used for flexural strength and fracture toughness tests with a loading span of 24 mm. The flexural strength measurement is performed at a cross-head speed of 0.5mm/min. The measurement of fracture toughness was carried out under a single-edge notched beam method at a cross-head speed of 0.05mm/min. Depth and width of single-edge notch size were 0.4 mm in length and 0.12 mm in width, respectively. The flexural strength and fracture toughness were calculated with the following formulas by averaging four individual measurement resultants, respectively.

$$\sigma = 3PL / (2bh^2) \quad (2)$$

$$K_{IC} = Y \times 3PLa^{1/2} / (2BW^2) \quad (3)$$

Where P is the breaking load of the specimen, and L, b, h, Y, and  $\alpha$  denote the span, width, height, form factor, and notch depth of the specimen, respectively.

The phase analysis was examined by the X-ray diffraction (XRD, D/max 2200PC, Rigaku, Japan) with a Cu K $\alpha$  radiation at 40 kV and 30 mA. Microstructure analysis of the samples was identified in a scanning electron microscopy (SEM, JSM-6700, JEOL Ltd, Japan) with an energy dispersive spectrometer (EDS, Be4-U92 of an analysis range, Oxford, Britain).

### 3. Results and discussion

#### 3.1 Phase identification and reaction mechanism

The reaction path in the vacuum hot press sintering of the as-milled powders is investigated by XRD with the purpose of reaction mechanism. The main phases components detected by the XRD at different hot pressing temperatures for 2 h are summarized in Fig. 1 for the sample with target 7.54 at.% Al<sub>2</sub>O<sub>3</sub> (No. b of Tab. I). It can be found that there is no evident reaction among Ti, Al, TiO<sub>2</sub>, Cr and V<sub>2</sub>O<sub>5</sub>, only the diffraction peaks of the initial materials (Ti, Al, TiO<sub>2</sub>, Cr and V<sub>2</sub>O<sub>5</sub>) are existed except for a very handful of TiAl<sub>3</sub> phases at 500 °C. The formation of a very little amount of TiAl<sub>3</sub> is closely related with diffusion reaction between Al and Ti, which implied that Al began to react with Ti to form TiAl<sub>3</sub> under the Al melting point at their crystal boundary. This result is in agreement well with the previous work [20].

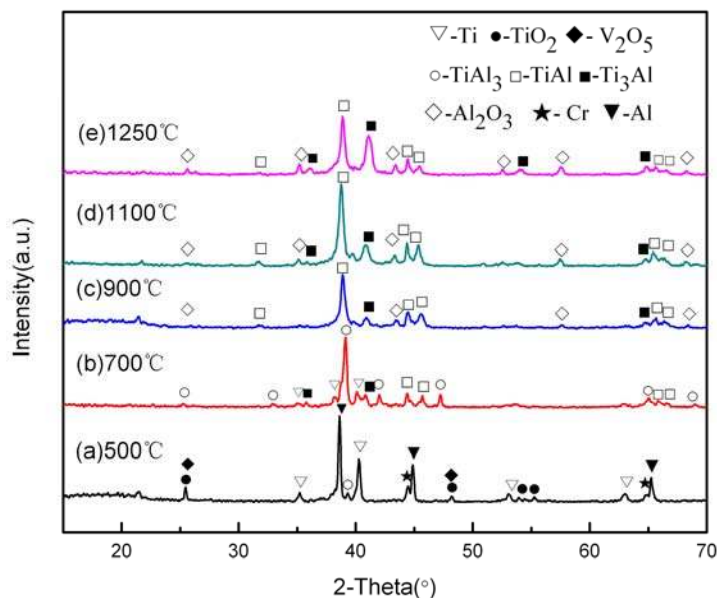


**Fig. 1** XRD patterns of composites fabricated at different temperatures with target 7.54 at.% Al<sub>2</sub>O<sub>3</sub>

It could be seen that there was much obvious feature change for the sample heated at 700 °C for 2h. The diffraction peaks of TiAl<sub>3</sub> increased evidently and became the main phase. Two new phases of TiAl and Ti<sub>3</sub>Al were detected associated with the decrease of the amount of initial materials (Ti, Al, TiO<sub>2</sub>, Cr and V<sub>2</sub>O<sub>5</sub>). The XRD results mentioned above reveal that the Ti-Al intermetallic compounds could have been formed after Al melts at about 660 °C.

Meanwhile  $\text{TiAl}_3$  phases were generated at surface of Ti grains by chemical reaction of liquid Al and solid Ti. As the reaction proceeded,  $\text{TiAl}_3$  and Ti reacted to form TiAl and  $\text{Ti}_3\text{Al}$  phases.

When the temperature increased to 900 °C, the as-sintering specimen mainly consists of  $\gamma$ -TiAl,  $\alpha_2$ - $\text{Ti}_3\text{Al}$ ,  $\text{Al}_2\text{O}_3$  phases. It is noted that the TiAl phase has been the main phase at 900 °C. The appearing of  $\text{Al}_2\text{O}_3$  phase is attributed to the thermit reaction of  $\text{TiO}_2$  and Al.

Although the variation in amount of phases for sample hot pressed at 1100 °C and 1250 °C shows mostly the same tendency as that at 900 °C, it can be seen that the diffraction peaks of  $\text{Ti}_3\text{Al}$  phases increase gradually and the TiAl phases first increase at 1100 °C then decrease at 1250 °C. It is also worth to note that the reflection peaks of TiAl ( $2\theta=38.900$ ) shift to large angles compared to the theoretical position of 38.470, which is attributed to the decrease of lattice parameters. The decrease of the lattice parameters is ascribed to the small size of V and Cr atom, which is in good agreement with previous result [21].

The existence of the above-mentioned phases in the composites formed in the temperature range from 500-1250 °C could be assumed as follows:

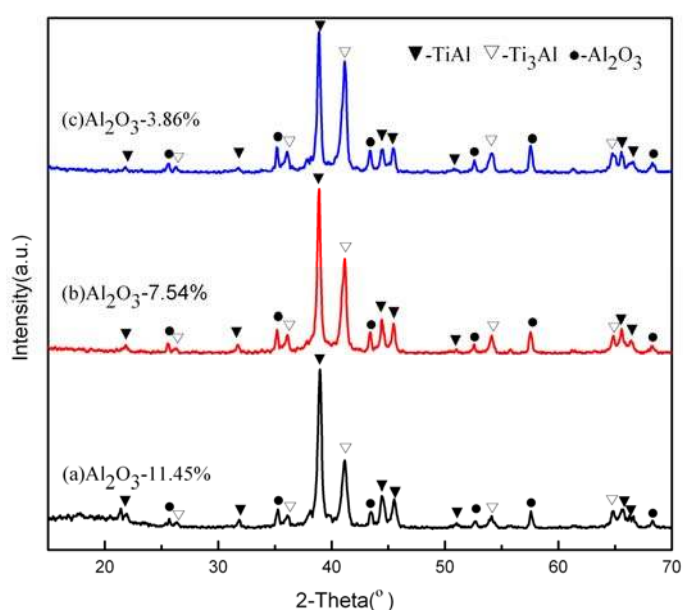


**Fig.2** XRD patterns of composites with various  $\text{Al}_2\text{O}_3$  contents hot pressed at 1250°C

Fig.2. shows the XRD patterns of the  $\text{Al}_2\text{O}_3/\text{TiAl}$  composites hot-pressed at 1250 °C for 2h with various target  $\text{Al}_2\text{O}_3$  contents. It can be clearly found that as-synthesized composites contain  $\gamma$ -TiAl,  $\alpha_2$ - $\text{Ti}_3\text{Al}$ ,  $\text{Al}_2\text{O}_3$  phases as three major phases and no any raw reagents existing. Compared with ref. [21], there is no obvious Laves  $\text{Ti}(\text{Al,Cr})_2$  of solid solution with addition of Cr, which further confirmed that Cr and V diffused into TiAl to form solid solution. Meanwhile, it is clear that the  $\alpha_2$ - $\text{Ti}_3\text{Al}/\gamma$ -TiAl ratio and the intensity of the  $\text{Al}_2\text{O}_3$  diffraction peaks increase with the increment of  $\text{Al}_2\text{O}_3$  content.

### 3.2 Microstructure characterization

Fig.3 shows the typical of fracture surface and EDS analysis of the sample with 7.54 at.%  $\text{Al}_2\text{O}_3$ . Although it is hard to quantitatively identify the amount of individual phase in the products, the fracture surface shows the as fabricated sample consisted of granular grains (white regions) and layered ones (dark regions). Further chemical composition characterization using EDS in Fig. 3 indicates that the granular grains is composed of Al and O elements with atomic ratio of 64.60:36.40, indicating that the granular grains are  $\text{Al}_2\text{O}_3$ , while the typical layered grain consists of Ti, Al, V and Cr are TiAl and  $\text{Ti}_3\text{Al}$ , in agreement with the XRD result given in Fig. 1 and Fig. 2. The  $\text{Al}_2\text{O}_3$  ceramic particles as reinforcement inclined to distribute homogeneously and randomly on the grain boundaries of the TiAl matrix.

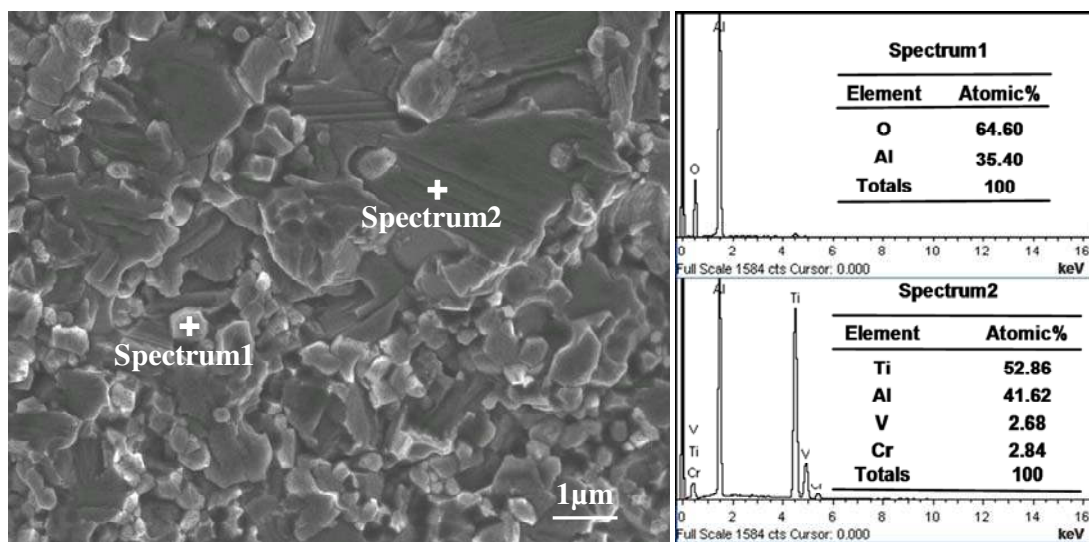


**Fig.3** EDS analysis of fracture surface of sample with 7.54 at.% target  $\text{Al}_2\text{O}_3$  content

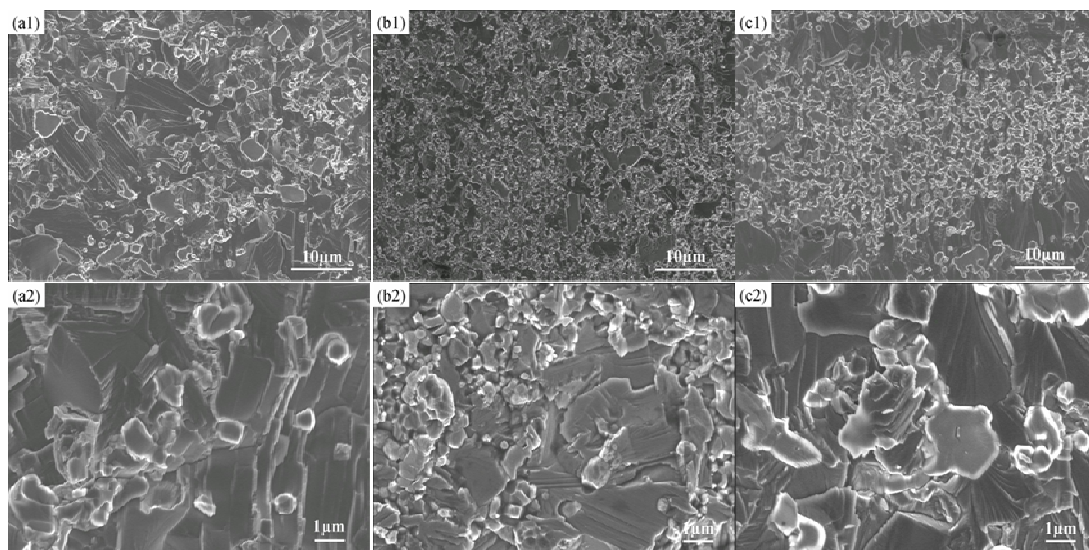


**Fig. 4** the SEM images of fracture surface of samples with different target contents of  $\text{Al}_2\text{O}_3$

Fig. 4 shows that the SEM images of fracture surface of samples with different target contents of  $\text{Al}_2\text{O}_3$ . It is evidently found that the content of  $\text{Al}_2\text{O}_3$  notably increases in sequence at the low magnification (a1-c1), which is in accordance with above XRD analysis in Fig. 2. The matrix grain size of the as synthesized  $\text{Al}_2\text{O}_3/\text{TiAl}$  composites decreased obviously as the  $\text{Al}_2\text{O}_3$  content increased, and the  $\text{Al}_2\text{O}_3$  particles changed from agglomerating (Fig. 4a) state to homogenization (Fig. 4b). These suggest that during the synthesis process of the  $\text{Al}_2\text{O}_3/\text{TiAl}$  composites the in situ formed  $\text{Al}_2\text{O}_3$  particles are much resistant to the grain growth of the matrix TiAl. However, when the  $\text{Al}_2\text{O}_3$  content was reached 11.45 at.%, the  $\text{Al}_2\text{O}_3$  particles tended to be agglomerate again, which were detrimental to the mechanical properties of the in situ  $\text{Al}_2\text{O}_3/\text{TiAl}$  composites.

### 3.3 Strengthening and toughening mechanisms

The strengthening effects are attributed to the combination effects of grain refining and  $\text{Al}_2\text{O}_3$  second phase. The strengthening effect of in situ formed fine  $\text{Al}_2\text{O}_3$  particles results in high resistance of deformation and residual stress toughening because of its high hardness and high modulus. Meanwhile, the microstructure was refined evidently with the increment of  $\text{Al}_2\text{O}_3$  second phase, which also play an important role in improving mechanical strength on the basis of Hall-Petch equation [22]. Finally, element V and Cr of solid solution could improve strength to some extent.

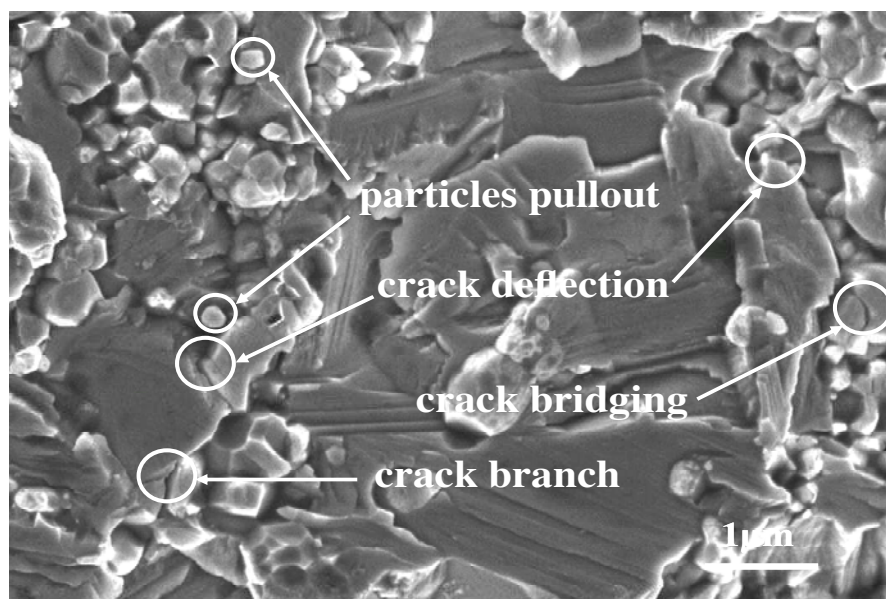


**Fig. 5.** Typical crack propagation patterns of  $\text{Al}_2\text{O}_3/\text{TiAl}$  composite with 7.54 at.%  $\text{Al}_2\text{O}_3$

The toughening mechanisms of as-synthesized  $\text{Al}_2\text{O}_3/\text{TiAl}$  composites could also explained by the typical [fracture](#) crack propagation paths pattern in Fig.5. It could be seen that various fracture mode of transgranular and intergranular fracture, particles pullout, crack bridging, crack deflection and branching coexisted in the  $\text{Al}_2\text{O}_3/\text{TiAl}$  in situ composites. The zigzag crack propagation is mainly due to dispersed fine  $\text{Al}_2\text{O}_3$ , showing crack propagation on several planes with tortuous routes, which interprets the increase of the flexural strength and fracture toughness. In addition, room temperature ductility and toughness are increase by adding V and Cr [19].

### 3.4 Physical and Mechanical Properties

Tab. II shows the physical and mechanical properties of the in situ Al<sub>2</sub>O<sub>3</sub>/TiAl composites with various content of Al<sub>2</sub>O<sub>3</sub>. The measured density of Al<sub>2</sub>O<sub>3</sub>/TiAl composites increases gradually from 3.97 to 4.02 g/cm<sup>3</sup> with the volume contents of Al<sub>2</sub>O<sub>3</sub> ranging from 3.86 to 11.45%, and all of them reaches 98-99% of the theoretical density. The hardness (HV) increase from 469.80 to 567.97 kg/mm<sup>2</sup>. The minor increase in density is attributed to the higher density (3.97 g/cm<sup>3</sup>) of in situ formed Al<sub>2</sub>O<sub>3</sub> density than that of 3.8 g/cm<sup>3</sup> for TiAl and finer microstructure with the increment of the content of Al<sub>2</sub>O<sub>3</sub>. The increase of hardness results from the high hardness of Al<sub>2</sub>O<sub>3</sub> (18 GPa) and the increment of the density of the Al<sub>2</sub>O<sub>3</sub>/TiAl in situ composites.

**Tab. II.** Physical and Mechanical Properties of the Al<sub>2</sub>O<sub>3</sub>/TiAl Composites with Different Target Al<sub>2</sub>O<sub>3</sub> Content

Sample s No.	Fracture toughness (MPa m <sup>1/2</sup> )	Flexural strength (MPa)	Density (g/cm <sup>3</sup> )	Vickers hardness (kg/mm <sup>2</sup> )
a	4.39	238.35	3.97	469.80
b	5.39	335.38	4.00	522.17
c	4.25	172.21	4.02	567.97

The values of the flexural strength and fracture toughness firstly enhanced with increase of target Al<sub>2</sub>O<sub>3</sub> content, and then dropped to a relative low point. Both the flexural strength and fracture toughness with 7.54 % Al<sub>2</sub>O<sub>3</sub> content possess peak values of 335.38 MPa and 5.39 MPa m<sup>1/2</sup>, respectively. Compared with the lowest property (3.86 % target Al<sub>2</sub>O<sub>3</sub> content), these values raised by 140.71% and for flexural strength and 122.78% for fracture toughness. The quantitative analysis of mechanical properties are consistent with the SEM results.

### 4. Conclusion

(1) Al<sub>2</sub>O<sub>3</sub>/TiAl composites were fabricated at 1250 °C by in situ synthesis and vacuum hot pressing based on the Ti-Al-TiO<sub>2</sub>-V<sub>2</sub>O<sub>5</sub>-Cr system. The as-synthesized composites mainly consisted of  $\gamma$ -TiAl,  $\alpha_2$ -Ti<sub>3</sub>Al, Al<sub>2</sub>O<sub>3</sub>.

(2) With 7.54 at.% Al<sub>2</sub>O<sub>3</sub> reinforcement, the flexural strength and fracture toughness of the as-sintered composite peaked of 335.38MPa and 5.39MPa m<sup>1/2</sup>, which respectively increased by 140.71% and 122.78% contrasted with 3.86 % target Al<sub>2</sub>O<sub>3</sub> content.

(3) The strengthening effects are attributed to grain refining and Al<sub>2</sub>O<sub>3</sub> second phase. The toughening mechanisms include crack bridging, crack deflection, branching and particles pullout.

### Acknowledgement

This work was supported by the National Foundation of Natural Science, China (51171096 50802057).

## 5. References

1. R. K. Shiue, S. K. Wu, S. Y. Chen, *Intermetallics* 12 (2004) 929.
2. Y. L. Li, P. He, J. C. Feng, *Scripta. Mater.* 55 (2006) 171.
3. T. Tetsui, *Intermetallics*. 9 (2001) 253.
4. M. Yamaguchi, H. Inui, K. Ito, *Intermetallics*. 48 (2000) 307.
5. X. H. Wu, *Intermetallics*. 14 (2006) 1114.
6. N. Forouzanmehr, F. Karimzadeh, M. H. Enayati, *J. Alloys. Compd.* 471 (2009) 93.
7. Couret, G. Molenat, J. Galy, M. Thomas, *Intermetallics*. 16 (2008) 1134.
8. P. Bhattacharya, P. Bellon, R. S. Robert, *J. Alloys. Compd.* 368 (2004) 187.
9. K. II. Moon, K. S. Lee, *J. Alloys. Compd.* 291 (1999) 312.
10. Z. W. Li, W. Gao, D. L. Zhang, Z. H. Cai, *Corros. Sci.* 46 (2004) 1997.
11. K. P. Rao, Y. J. Du, *Mater. Sci. Eng. A* 277 (2000) 46.
12. B. C. Mei, Y. Miyamoto, *Mater. Chem. Phys.* 75 (2007) 291.
13. D. E. Alman, *Intermetallics*. 13 (2005) 572.
14. W. K. Zhang, L. Z. Gao, Y. Lei, B. J. Yang, L. Xiao, Y. S. Yin, *Mater. Sci. Eng. A* 527 (2010) 7436.
15. N. Forouzanmehr, F. Karimzadeh, M. H. Enayati, *J. Alloys. Compd.* 478 (2009) 257.
16. Y. H. Wang, J. P. Lin, Y. H. He, Y. L. Wang, G. L. Chen, *J. Alloys. Compd.* 468 (2009) 505.
17. Y. Choi, S. W. Rhee, *J. Mater. Sci.* 28 (1993) 6669.
18. Gotman, M. J. Koczak, E. Shtessel, *Mater. Sci. Eng. A* 187 (1994) 189.
19. J. P. LIN, L. Q. ZHANG, X. P. Song, F. Ye, G. L. Chen, *Mater. China.* 29 (2010) 1.
20. R. Martin, *Metall. Mater. Trans. A* 33 (2002) 2747.
21. L. Y. Xiang, F. Wang, J. F. Zhu, X. F. Wang, *Mater. Sci. Eng. A* 528 (2011) 3337.
22. F. Whitehouse, T. W. Clyne, *Composites*. 24 (1993) 256.

---

**Садржај:**  $Al_2O_3/TiAl$  композити допирани са  $Cr$  и  $V_2O_5$  успешно су синтетизовани из  $Ti$ ,  $Al$ ,  $TiO_2$ , методом топлог пресовања. Испитиван је утицај тренутног формирања фазе  $Al_2O_3$  на фазни састав, микроструктуру и механичка својства композита  $Al_2O_3/TiAl$ . Резултати су показали да се тако синтетизован композит састоји углавном из матрикса  $\gamma-TiAl/\alpha_2-Ti_3Al$  и дисперзно ојачане фазе  $Al_2O_3$ . Тренутно формиране fine  $Al_2O_3$  керамичке честице су дисперговане по границама зрна  $TiAl$ , резултујући пречишћавањем  $TiAl$  матрикса, што даље доприноси побољшању механичких својстава композита  $Al_2O_3/TiAl$ . Композит са 7,54 at.%  $Al_2O_3$  показује максималан модул отпорности и жилавост лома од 335,38 МПа и 5,39 МПа  $m^{1/2}$ , истим редоследом. Механизам јачања је такође детаљно продискутован.

**Кључне речи:**  $TiAl$  композит,  $Al_2O_3$ , микроструктура, механичка својства.

---